

**Models for quasi-two-dimensional helium and magnets\***

David N. Lambeth<sup>†</sup> and H. Eugene Stanley

*Physics Department, Massachusetts Institute of Technology, Cambridge, Massachusetts 02139*

(Received 4 April 1973; revised manuscript received 26 March 1975)

Recently considerable interest has focused upon materials which change spatial dimensionality as the anisotropy parameter  $R$  is varied. Here we calculate the high-temperature series of the two-spin correlation function for the classical Heisenberg ( $D = 3$ ) and planar ( $D = 2$ ) models with lattice anisotropy. The Hamiltonian is

$$\begin{aligned} \mathcal{H} &= -J_{xy} \sum_{\langle ij \rangle}^{xy} \vec{S}_i^{(D)} \cdot \vec{S}_j^{(D)} - J_z \sum_{\langle ij \rangle}^z \vec{S}_i^{(D)} \cdot \vec{S}_j^{(D)} \\ &= -J_{xy} \left( \sum_{\langle ij \rangle}^{xy} \vec{S}_i^{(D)} \cdot \vec{S}_j^{(D)} + R \sum_{\langle ij \rangle}^z \vec{S}_i^{(D)} \cdot \vec{S}_j^{(D)} \right) \end{aligned}$$

where  $\vec{S}_i^{(D)}$  is a classical spin of  $D$  dimensions, the first summation is over all nearest-neighbor pairs in the  $xy$  plane, and the second sum is over pairs of spins coupling adjacent planes. The two-spin correlation functions are used to obtain the susceptibility ( $\chi$ ), specific heat ( $C_H$ ) and spherical moments ( $\mu_t$ ) as double power series in  $J_{xy}/k_B T$  and  $J_z/k_B T$  on both the simple-cubic and face-centered-cubic lattices. All series are to tenth order except for the Heisenberg model on the simple-cubic lattice which is to ninth order. The family of  $n$ th derivatives with respect to  $R$  are analyzed for the susceptibility and the spherical moments. By considering these functions in the limit  $R = 0$ , we obtain evidence concerning the possibility of a phase transition for the two-dimensional ( $d = 2$ ) lattice. Our evidence rests upon standard methods, as well as on two new sequences (based on scaling in the parameter  $R$ ):  $\Delta_{n,l} \equiv \rho_{n,l} - \rho_{n-1,l} \sim \varphi T_c / l T_c^{MF}$  and  $\bar{\Delta}_{n,l} \equiv n \rho_{n-1,l} - (n-1) \rho_{n,l} \sim (T_c/T_c^{MF})[(\gamma_0 - 1)/l + 1]$ . Here  $\rho_{n,l} \equiv (a_{l+n,n} a_{l+n-1,n})/a_{l,0}$ , where  $a_{l,n}$  are the coefficients in  $\bar{\chi}^{(n)} \equiv \partial^n \bar{\chi} / \partial R^n \propto \sum_{l=n}^{\infty} a_{l,n} (J_{xy}/k_B T)^l$ . Much of the evidence for the cases considered in this work ( $D = 2, 3$ ) is strengthened by comparison with the exactly known situations  $D = 1$  (Ising model) and  $D = \infty$  (spherical model). Subject to the assumption that scaling in  $R$  holds, we estimate that the susceptibility exponent for the classical planar model is  $\gamma_0(D = 2) = 2.53^{+0.30}_{-0.28}$ . The evidence for the Heisenberg model is not as convincing, but if a phase transition does exist, then our methods suggest a susceptibility exponent of  $\gamma_0(D = 3) \cong 3.5$ .

I. INTRODUCTION

Onsager's<sup>1</sup> quadratic-lattice Ising model, which concerns a one-dimensional ( $D = 1$ ) spin space, has a critical point located at  $T_c/T_c^{MF} = 0.5667$ , where  $T_c^{MF}$  is the mean-field-theory critical temperature. Yet the quadratic-lattice spherical model,<sup>2a</sup> which has been shown to be equivalent to an infinite-dimensional ( $D = \infty$ ) spin space,<sup>2b</sup> exhibits no phase transition, i. e.,  $T_c = 0$ . Hence the natural question arises: At what value of  $D$  does the phase transition disappear?

Since  $D > 3$  has not been shown to correspond to any real material, we will concern ourselves only with the question: Does the phase transition exist only for  $D = 1$  or does it persist for  $D = 2$  or  $D = 3$ ?<sup>3-11</sup> The value of  $D = 3$ , corresponding to the classical Heisenberg model, is of particular interest, since as isotropic three dimensional spin space has been used for many years to describe magnetic systems. Also of importance is the  $D = 2$  case, the classical planar model, which corresponds to helium near the  $\lambda$  point.<sup>3</sup>

Mermin and Wagner<sup>4</sup> adopted a technique of Hohenberg,<sup>5</sup> which uses the Bogoliubov inequality,<sup>6</sup> to

show rigorously that there cannot be any spontaneous magnetization for  $D = 2$  and  $D = 3$  for a two-dimensional ( $d = 2$ ) lattice. This naturally leads one to doubt that the phase transition could occur at all. But as Stanley and Kaplan<sup>7</sup> pointed out, this behavior does not preclude the existence of a phase transition. Perhaps other physical quantities will show a singularity at  $T > 0$  even though the spontaneous magnetization does not. After analyzing high-temperature series of the susceptibility of various two-dimensional lattices for the classical Heisenberg ( $D = 3$ ) and, later, the planar<sup>8</sup> ( $D = 2$ ) models, it was proposed that the susceptibility diverged at a nonzero critical temperature. Moore<sup>9</sup> obtained additional evidence for the plane triangular lattice by extending the series and by analyzing the spherical moments

$$\mu_t \equiv \sum_{\vec{r}} |\vec{r}|^t C_2(\vec{r}), \tag{1.1}$$

where  $C_2(\vec{r})$  is the spatial two-spin correlation function. He reasoned that  $\mu_t$ , especially for  $t < 0$ , might be a better quantity to study than the susceptibility ( $t = 0$ ), since the two-spin correlation functions far from the origin weight the lattice counting

more strongly than the effects of the Hamiltonian.

Further evidence for the existence of a phase transition was put forth by Mubayi and Lange.<sup>10a</sup> Developing a Green's-function decoupling to describe the thermodynamic behavior of the spin- $\frac{1}{2}$  Heisenberg model, they found that not only did the static susceptibility diverge [as  $1/(T - T_c)$ , where  $T_c = 2J/k_B$ ], but that the spontaneous magnetization remained zero for all  $T > 0$  (consistent with Mermin and Wagner<sup>4</sup>). Still one might have doubts that the transition actually occurs, especially in light of how much the divergence looks like mean-field behavior. (In mean-field theory a transition exists for all spatial dimensions.) To overcome the fact that some decouplings appear to give a transition and others do not, Oguchi<sup>10b</sup> has recently applied a variational technique to the antiferromagnet and reproduced analogs of the Mubayi-Lange results. Additional support of a phase transition has been put forth by Berezinskii<sup>11</sup> by considering low-temperature expansions with an external field.

In the present study we investigate the planar ( $D=2$ ) and the classical Heisenberg ( $D=3$ ) models using high-temperature series for the two-spin correlation functions. We employ the concepts of "scaling"<sup>12</sup> and "crossover"<sup>13</sup> when a system with lattice anisotropy (different coupling strengths in different lattice directions) changes universality classes. In Sec. II we describe the Hamiltonian which is used to study the two-dimensional behavior. Also discussed are the predictions of scaling and the consequences they have on this problem. In Sec. III we describe the series expansions and comment on their accuracy. Contained in Sec. IV is a discussion of the methods of analysis used to study the high-temperature series presented in the Appendix. Here we propose two new methods of obtaining the critical indices. Included with the methods of analysis are discussions pertinent to the results of each method. Finally, in Sec. V we present our conclusions.

## II. MODELS AND SCALING PREDICTIONS

We define the Hamiltonian for a  $d=3$  lattice with anisotropy as

$$\begin{aligned} \mathcal{H} &= -J_{xy} \sum_{\langle ij \rangle} \vec{S}_i^{(D)} \cdot \vec{S}_j^{(D)} - J_z \sum_{\langle ij \rangle} \vec{S}_i^{(D)} \cdot \vec{S}_j^{(D)} \\ &= -J_{xy} \left( \sum_{\langle ij \rangle} \vec{S}_i^{(D)} \cdot \vec{S}_j^{(D)} + R \sum_{\langle ij \rangle} \vec{S}_i^{(D)} \cdot \vec{S}_j^{(D)} \right), \end{aligned} \quad (2.1)$$

where  $\vec{S}_i^{(D)}$  is the  $D$ -dimensional classical spin ( $D=1, 2, 3$ , and  $\infty$  are the Ising, classical planar, classical Heisenberg, and spherical models, respectively) located at the  $i$ th site of the lattice. The first summation is restricted to nearest-neighbor (nn) pairs of spins which lie in a common  $xy$  plane while the second summation is over nn pairs

of spins whose relative displacement vector has a  $z$  component. The quantity  $R \equiv J_z/J_{xy}$  is the ratio of interplanar to intraplanar coupling strengths and is referred to as the anisotropy parameter.

As  $R \rightarrow 0$  in the Hamiltonian (2.1), the critical behavior crosses over from that of a three-dimensional lattice to that of a two-dimensional lattice. Scaling theory<sup>12,13</sup> predicts that the critical temperature  $T_c(R)$  varies with  $R$  for small  $R$  as

$$T_c(R) - T_c(0) \sim R^{1/\phi}, \quad (2.2)$$

where  $\phi$  is the crossover exponent and  $T_c(0)$  is the critical temperature for the two-dimensional lattice. Furthermore, physical quantities such as the susceptibility

$$\bar{\chi} = \sum_{\vec{r}} C_2(\vec{r}) \quad (2.3)$$

can be expanded as a power series in  $R$

$$\bar{\chi} \sim \sum_{n=0}^{\infty} f_n R^n, \quad (2.4)$$

where the coefficients  $f_n$  are given by

$$f_n \sim \left( 1 - \frac{T_c(0)}{T} \right)^{-\gamma_n} \quad (2.5)$$

and

$$\gamma_n = \gamma_0 + n\phi, \quad (2.6)$$

where  $\gamma_0$  is the two-dimensional susceptibility exponent. Hence by differentiating  $\bar{\chi}$  with respect to  $R$  and allowing  $R$  to go to zero, we obtain

$$\left. \frac{\partial^n \bar{\chi}}{\partial R^n} \right|_{R=0} \sim \left( 1 - \frac{T_c(0)}{T} \right)^{-\gamma_n} \quad (2.7)$$

This functional form is easily derived using the generalized homogeneous function approach to scaling.<sup>13,14</sup> It is important to point out that other quantities (such as  $\mu_t$  and specific heat) show similar crossover behavior when derivatives with respect to  $R$  are taken. Of particular interest for this paper are the spherical moments, Eq. (1.1), for which

$$\left. \frac{\partial^n \mu_t}{\partial R^n} \right|_{R=0} \sim \left( 1 - \frac{T_c(0)}{T} \right)^{-\nu_n(t)}, \quad (2.8)$$

where

$$\nu_n(t) = t\nu_0 + \gamma_0 + n\phi, \quad (2.9)$$

and where  $\nu_0$  is the two-dimensional correlation-length exponent.

For the spin- $\frac{1}{2}$  Ising model ( $D=1$ ), where  $T_c(0)$  is known exactly,<sup>1</sup> various other studies<sup>14-17</sup> have been performed on  $\bar{\chi}$ ,  $\mu_2$ , and the reduced specific heat  $\bar{C}_H$ . After some initial disagreement,<sup>16,17</sup> it is now believed that scaling with a parameter holds for lattice dimensionality crossover.<sup>14</sup> Furthermore, it is believed that the crossover exponent  $\phi$

is equal to the two-dimensional susceptibility exponent  $\gamma_0$ . In fact, Liu and Stanley have shown

$$\left. \frac{\partial \bar{\chi}}{\partial R} \right|_{R=0} \propto [\bar{\chi}(0)]^2 \quad (2.10)$$

for all values of the spin dimensionality  $D$ .<sup>18</sup> Hence they have demonstrated that  $\gamma_1 = 2\gamma_0$ . They have also shown for the Ising model that the  $n=2$  and  $n=3$  derivatives of  $\bar{\chi}$  and  $\mu_2$  are bounded on both sides by the two-dimensional quantities  $\bar{\chi}(0)$  and  $\mu_2(0)$  raised to powers. For example, on the simple cubic lattice,

$$\left( \frac{2J_{xy}}{k_B T} \right)^2 [\bar{\chi}(0)]^3 \leq \left. \frac{\partial^2 \bar{\chi}}{\partial R^2} \right|_{R=0} \leq 2 \left( \frac{2J_{xy}}{k_B T} \right)^2 [\bar{\chi}(0)]^3. \quad (2.11)$$

This clearly indicates that, at the very least, one can expect the derivatives to have the same critical temperature. Although the inequality necessary to derive the bounding relationships has been derived only for the  $D=1$  case,<sup>19</sup> one should not conclude that similar inequalities for the higher spin dimensions will not eventually be proved.

### III. SERIES

Using the renormalized linked-cluster expansion theory of Wortis, Jasnow, and Moore,<sup>20</sup> the two-spin correlation functions  $C_2(\vec{r})$  were obtained as power series in inverse temperature for a judiciously chosen set of  $J_{xy}$  and  $J_z$  values. The pertinent physical quantities were found for each of the  $(J_{xy}, J_z)$  values. These quantities were then obtained as double power series in  $J_{xy}/k_B T$  and  $R \equiv J_z/J_{xy}$  by solving a system of simultaneous equations using the set of expansions for particular  $J_{xy}$  and  $J_z$  values as known. From  $C_2(\vec{r})$  the reduced susceptibility

$$\bar{\chi}(J_{xy}, J_z) \equiv \frac{k_B T \chi}{N \mu^2} = \sum_{\vec{r}} C_2(\vec{r}), \quad (3.1)$$

various spherical moments  $\mu_t$ , and the reduced specific heat

$$\bar{C}_H(J_{xy}, J_z) \equiv \frac{TC_H}{N} = -\frac{1}{2} T \frac{\partial}{\partial T} \sum_{\vec{r}} J_{\vec{r}} C_2(\vec{r}) \quad (3.2)$$

are obtained. Here  $J_{\vec{r}}$  corresponds to the nn interactions  $J_{xy}$  and  $J_z$ .

The general- $R$  expansions take the form

$$\bar{\chi} = \sum_{n=0}^{\infty} \sum_{j=0}^n a_{nj} \left( \frac{J_{xy}}{k_B T} \right)^n R^j, \quad (3.3)$$

$$\mu_t = \sum_{n=0}^{\infty} \sum_{j=0}^n b_{nj}(t) \left( \frac{J_{xy}}{k_B T} \right)^n R^j, \quad (3.4)$$

and

$$\bar{C}_H = k_B T \sum_{n=2}^{\infty} \sum_{j=0}^n c_{nj} \left( \frac{J_{xy}}{k_B T} \right)^n R^j. \quad (3.5)$$

Since the specific heat has contributions only from the  $nm$  correlation functions, a large number of the double-power-series coefficients  $c_{nj}$  are identically

zero. For the sc lattice  $c_{nj} \equiv 0$  if  $j$  or  $n$  is odd, while the fcc lattice requires  $c_{nj} \equiv 0$  only for  $j$  odd. Because  $C_H$  involves a derivative with respect to temperature, the effective order of the expansion in  $1/k_B T$  is one larger than the order of  $\chi$ . Hence if it were not for the fact that  $c_{nj} \equiv 0$  for  $j$  odd, an extra set of  $(J_{xy}, J_z)$  values would be required in order to solve the system of simultaneous equations.

Tables I-III and the Appendix contain the general- $R$  series coefficients for  $\bar{\chi}^{\text{fcc}}$ ,  $\bar{\chi}^{\text{sc}}$ ,  $\mu_t^{\text{fcc}}$ ,  $\mu_t^{\text{sc}}$ ,  $\bar{C}_H^{\text{fcc}}$ , and  $\bar{C}_H^{\text{sc}}$  for  $D=1, 2, 3$ , and  $\infty$ .

There are some interesting tests that can be performed on the general- $R$  polynomials to check their accuracy. (a) As  $R$  approaches zero, the coefficients must take on their two-dimensional values. While these expansions are to a higher order than previously calculated for the square (quadratic) lattice, the known coefficients agree with our results.<sup>7,8</sup> (b) When  $R = \infty$  (i. e.,  $J_z = 1$  and  $J_{xy} = 0$ ) the diagonal elements of the simple cubic polynomials are the linear chain coefficients while the diagonal elements of the face-centered-cubic polynomials are the body-centered-cubic coefficients.<sup>21</sup> (c) The isotropic three-dimensional coefficients are obtained by setting  $R=1$ , that is, by summing the coefficients in the tables horizontally for the sc and fcc lattices result.<sup>21</sup>

Additional checks that measure the accuracy of the coefficients utilize rigorous proofs developed by Liu and Stanley,<sup>18</sup>

$$\bar{\chi}^{(1)} = g(J_{xy}/k_B T) (\bar{\chi}^{(0)})^2 \quad (3.6)$$

and

$$\mu_2^{(1)} = g(J_{xy}/k_B T) [(\bar{\chi}^{(0)})^2 + 2\bar{\chi}^{(0)} \mu_2^{(0)}], \quad (3.7)$$

where the superscript again equals the number of derivatives with respect to  $R$ , and where  $g$  is the number of out-of-plane nn bonds ( $g=2$  and  $g=8$  for the sc and fcc, respectively). These relationships are true for any two-sublattice structure which is connected by an anisotropy parameter. Hence there is a similar set of equations for the linear chain limit of the sc problem. The difference is that  $g=4$  and the derivatives are taken with respect to  $1/R$ . (We have also found these relationships useful in checking series involving second-nearest neighbors.<sup>22</sup>)

We have solved the simultaneous equations both with and without the use of (3.6) and (3.7). Hence by comparing the two sets of solutions we have an estimate of the accuracy of the coefficients. We believe that due to computer roundoff and the general approach of obtaining polynomials by solving simultaneous equations, the number of accurate significant digits is approximately

$$(\text{number significant digits}) \cong 19 - n - D. \quad (3.8)$$

TABLE I. Coefficients  $a_{nj}$  in the reduced susceptibility series for the classical Heisenberg model on the fcc lattice,

$$\bar{\chi} = \frac{k_B T \chi}{N \mu^2} = \sum_{n=0}^{\infty} \sum_{j=0}^{\infty} a_{nj} (\beta J_{xy})^n R^j.$$

$n \setminus j$	0	1	2	3	4	5	6	7	8	9	10
0	1										
1	4	8									
2	12	64	56								
3	33.6	320	656	387.2							
4	85.6	1305.6	4531.2	5952	2580.8						
5	206.8571429	4 672	24 185.6	52 163.84	49 125.12	17 085.71429					
6	480.8228571	15 239.31429	109 799.3629	343 009.280	521 311.3600	387 450.880 0	111 399.6800				
7	1077.558857	46 398.90286	444 551.8629	1 878 071.259	4 071 752.741	4 821 763.730	2 932 658.8263	723 335.8263			
8	2349.243429	133 748.736 0	1 650 623.049	9 027 475.162	26 081 258.50	43 571 681.17	41 869 288.91	21 673 374.28	4 658 268.005		
9	4 978.286545	368 694.950 3	5 723 226.127	39 305 961.09	144 910 237.3	319 306 555.8	429 612 834.1	348 990 245.0	156 538 918.2	29 914 360.36	
10	10 324.948 40	978 697.375 6	18 764 183.90	158 215 124.2	722 270 748.2	2 011 098 819.	3 543 939 896.	4 006 658 401.	2 806 377 051.	1 114 006 834.	191 123 472.4

TABLE II. Coefficients  $b_{nj}$  in the second moment series for the planar model on the sc lattice,

$$\mu_2 \equiv \sum_{\vec{r}} |\vec{r}|^2 C_2(\vec{r}) = \sum_{n=0}^{\infty} \sum_{j=0}^{\infty} b_{nj} (\beta J_{xy})^n R^j.$$

$n \setminus j$	0	1	2	3	4	5	6	7	8	9	10
0	0										
1	4	2									
2	32	32	8								
3	162	272	128	17							
4	672	1680	1 248	336	24						
5	2459.333333	8544	9100	3892	640	23.66666667					
6	8257.333333	38 042.66667	54 848.	33 552	9088	922.6666667	15.33333333				
7	26 012.416 67	153 601.333 3	287 078	236 593	93 241	16 822	1 013.333 333	4.041 666 667			
8	77 996	575 107.333 3	1 351 077.333	1 437 104	768 088	205 522.6667	24 298.666 67	816.666 666 7	-3.666 666 667		
9	224 745.8833	2 027 392.667	5 843 322.5	7 775 255.667	5 379 749	1 984 560.333	369 267	28 412.833 33	410.666 666 7	-4.975 000 060	
10	626 693.577 8	6 802 476.4	23 604 497.34	38 343 885.96	33 223 346.11	16 017 778.52	4 215 454.108	547 616.624 9	25 933.339 94	7.066 665 708	-2.077 778 257

TABLE III. Coefficients  $c_{nj}$  in the reduced specific-heat series for the classical Heisenberg model on the sc lattice. Note that  $c_{nj}=0$  for  $j$  odd or  $n$  odd.

$$\bar{C}_H \equiv \frac{TC_H}{N} = k_B T \sum_{n=2}^{\infty} \sum_{j=0}^n c_{nj} (\beta J_{xy})^n R^j.$$

$n \setminus j$	0	2	4	6	8	10
2	2	1				
4	84	24	-1.8			
6	-6,857 142 857	468	-12	2,571 428 571		
8	-55,024	3 985.92	1899.072	-1.28	-3.24	
10	-204,517 403	29 099,725 71	55 231,817 5	453,394 281 3	13,371 429 95	3,787 012 794

Here  $n$  is the corresponding order of the high-temperature series coefficient. Hence for a tenth-order coefficient of the Heisenberg model ( $D=3$ ) the number of significant digits is approximately six. As there are variations in the accuracy of the coefficients depending on the lattice and on the power of  $R$ , Eq. (3.8) should not be relied upon too strongly.

In Sec. IV the coefficients will be used to test the concept of scaling and whether or not there is a nonzero  $T_c$  for  $R=0$ . Furthermore, the numbers may be used to shed light upon certain antiferromagnetic structures.<sup>23</sup> Also, it is hoped that the Heisenberg series will be of some help in understanding layered magnetic compounds<sup>24</sup> ( $R$  small), especially with respect to specific-heat data,<sup>25</sup> and that the planar model series will be of some use to the thin-film liquid-helium experimentalist.

#### IV. SERIES ANALYSIS AND RESULTS

In the Appendix<sup>26</sup> high-temperature series for the susceptibility, second moment, and specific heat for the planar and classical Heisenberg models on both the sc and the fcc lattices are presented. In addition, the same series for the spin- $\frac{1}{2}$  Ising model<sup>27</sup> have been published. All of these series, along with various spherical moments  $\mu_t$  ( $t < 0$ ) for all three models ( $D=1, 2$ , and  $3$ ), have been analyzed using the traditional methods of ratio tests<sup>28</sup> and Padé approximants (PA's).<sup>28-30</sup> In addition, two new sequences applicable to the cross-over problems are developed and discussed.

With the large number of series and methods of analysis available, more information has been accumulated than can be presented here. In the following paragraphs we show representative results and discuss other pertinent analysis.

##### A. Ratio tests

Consider a finite series, e.g., the susceptibility

$$\bar{\chi} \approx \sum_{l=0}^L A_l \left( \frac{J_{xy}}{k_B T} \right)^l, \quad (4.1)$$

with

$$A_l \equiv \sum_{j=0}^l a_{l,j} R^j; \quad (4.2)$$

then the  $n$ th derivative with respect to  $R$ , evaluated at  $R=0$ , is given by

$$\begin{aligned} \bar{\chi}^{(n)} &\approx n! \sum_{l=n}^L a_{l,n} \left( \frac{J_{xy}}{k_B T} \right)^l \\ &= n! \left( \frac{J_{xy}}{k_B T} \right)^n \sum_{l=0}^{L-n} a_{l+n,n} \left( \frac{J_{xy}}{k_B T} \right)^l. \end{aligned} \quad (4.3)$$

The ratios  $\rho_{n,l}$  are defined by

$$\rho_{n,l} \equiv a_{l+n,n} / a_{l,n}, \quad l=1, \dots, L-n. \quad (4.4)$$

Assuming that

$$\bar{\chi}^{(n)} \sim (1 - T_c/T)^{-\gamma_n}, \quad (4.5)$$

and performing the customary Taylor series expansion on Eq. (4.5), we find

$$\rho_{n,l} = (T_c/T_c^{\text{MF}})^{\gamma_{n-1}/l+1}. \quad (4.6)$$

Here the mean-field critical temperature for the  $d=2$  lattice is given by  $T_c^{\text{MF}} = J_{xy}/k_B a_{1,0}$ . By plotting the ratios versus  $1/l$ , a set of curves that should, for all  $n$ , intercept at  $T_c/T_c^{\text{MF}}$  is obtained. Furthermore, since the scaling hypothesis predicts that  $\gamma_n$  [Eq. (2.6)] should increase with  $n$  in constant increments of  $\phi$ , the slopes of each of these curves should increase by  $\phi T_c/T_c^{\text{MF}}$ .

In Fig. 1, ratio plots for the Ising, planar, and classical Heisenberg models for the first five  $R$  derivatives to the  $\bar{\chi}^{\text{fcc}}$  series<sup>31</sup> are presented. The similarities between the sets of ratios are consistent with the scaling predictions. There are a few differences, though. For the zeroth and the first  $R$  derivatives of the Ising-model series, a considerable amount of oscillation occurs in the ratios. This is in contrast to the ratios of the other models which show less oscillatory behavior and more of a slight downward curvature. In fact, it is this curvature which might lead one to speculate that the ratios for these models are going to turn downward and eventually oscillate wildly as do the two-dimensional spherical model ratios. However, downward curvature is not sufficient to argue against a phase

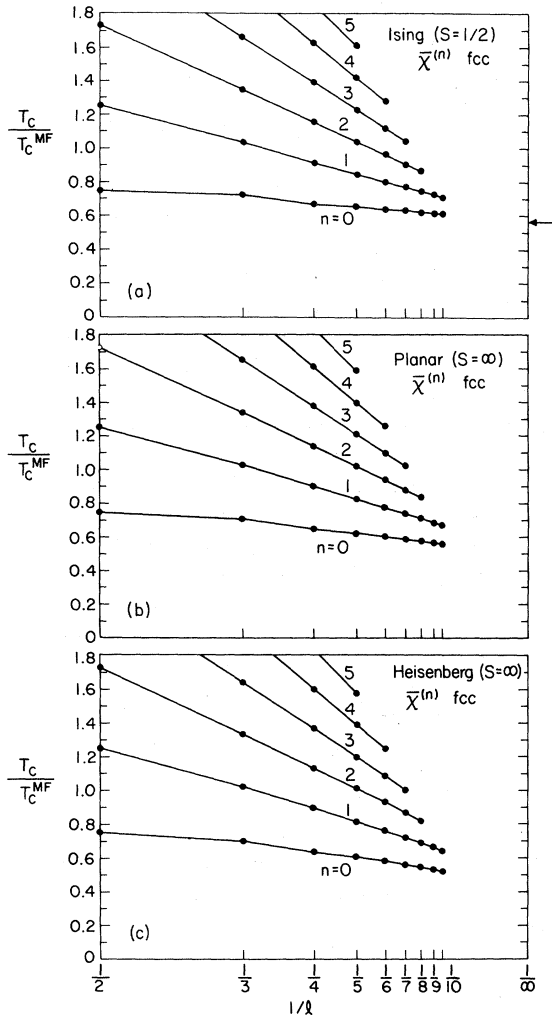


FIG. 1. Series ratios defined in Eq. (4.6) are plotted for  $\bar{\chi}^{\text{fcc}}$  for the (a) Ising, (b) planar, and (c) classical Heisenberg models (see Ref. 14). The arrow indicates the exact value for  $D=1$ .

transition. For a good example of *extreme curvature with a critical point one need only look at the three-dimensional spherical model series*. The higher-order derivatives ( $n \geq 2$ ) are similar for  $D=1, 2$ , and  $3$ , but  $D=2$  and  $D=3$  are still slightly different from the  $D=1$  ratios.<sup>32</sup> These curves for larger  $n$  ( $n \geq 2$ ) all seem to be much smoother than those for smaller  $n$ . This is as expected, since these series are sampling much more of the three-dimensional lattice.

It is not clear that the ratios should be plotted in the manner shown in Fig. 1. For the higher-order  $R$  derivatives ( $n > 0$ ), a factor of  $(J_{xy}/k_B T)^n$  [cf. Eq. (4.3)] can be extracted from the series. Where the ratios are skewed to the left they are referred to as "left-hand justified" (LHJ). It is equally correct to plot the ratios beginning at  $l=n$ , since both

plots should converge to  $T_c/T_c^{\text{MF}}$ . The second method of plotting is referred to as "right-hand justified" (RHJ). Since for a finite series it is not clear which method will show the most rapid convergence, both LHJ and RHJ methods have been investigated.

The ratios alone (Fig. 1) are not sufficient to predict an accurate value for the critical point. Not even with the addition of the various spherical moments [Eq. (1.1)] do the ratio plots by themselves give a good estimate for  $T_c$ . However, it can be added that ratio tests of all the possible series yield consistent results and seem to indicate the possibility that  $T_c^{(D)} \neq 0$  for  $D=2$  and  $D=3$ .

### B. Linear extrapolants

As mentioned earlier, Moore<sup>9</sup> found for the triangular lattice that the linear extrapolants

$$\mathcal{L}_{n,l}(t) \equiv l\rho_{n,l}(t) - (l-1)\rho_{n,l-1}(t) \quad (4.7)$$

seemed to be turning upward toward a nonzero  $T_c/T_c^{\text{MF}}$  for values of  $t < 0$ . Even though the  $\mathcal{L}_{0,l}(t)$  were not behaving particularly smoothly, Moore was able to interpret the trends of the extrapolants as pointing toward a nonzero critical temperature.

This method has also been used in our study, and somewhat similar results are seen for the quadratic lattice limit. Considering values of  $t$  down to  $t = -2$  it was found that the linear extrapolants for the planar model were turning up. However, this is nowhere as pronounced as for the more tightly packed triangular lattice.<sup>9</sup>

On the other hand, only a hint of the desired upward curvature can be seen for the oscillating Heisenberg ( $n=0$ ) linear extrapolants. This is in contrast to the Ising model spherical moments, which in spite of showing the oscillatory behavior of the ratios, always seem to converge to the known  $T_c$ . The extrapolants for higher  $R$  derivatives ( $n > 1$ ) are more independent of the model and appear almost always to be approaching the anticipated  $T_c$  from above (hence with slight downward curvature).

### C. Padé approximants

If one forms the logarithmic derivative to the series, Padé approximants (PA's) will give independent estimates for the critical indices. In Table IV, PA's for  $T_c/T_c^{\text{MF}}$  and  $\gamma_n$  for the first five  $R$  derivatives to the  $\bar{\chi}^{\text{fcc}}$  series for the planar model are shown. Of interest here is that while the estimates for  $T_c/T_c^{\text{MF}}$  are unsettled for  $n=1$  and  $n=2$ , they seem to be converging for  $n > 2$ . Also, the values given for  $\gamma_n$  are, as expected, increasing with regular increments. However, these increments are not constant enough to make good estimates for  $\phi$  (i. e.,  $\gamma_0$ ). While the PA's using the second moment series, as well as the negative

TABLE IV. Padé approximants (PA's) for the logarithmic derivatives to the first five  $\bar{\chi}^{(n)}$  series are shown for the planar model ( $D=2$ ). Using this method, independent estimates for  $T_c/T_c^{\text{MF}}$  (upper number) and  $\gamma_n$  (lower number) are obtained. The zeroth  $R$ -derivative table is not shown because the PA's for  $T_c/T_c^{\text{MF}}$  and  $\gamma_0$  are identical and one-half the values, respectively, of the  $n=1$  table values. This is a consequence of Eq. (3.6). Note that for larger  $n$  the  $T_c/T_c^{\text{MF}}$  values are more convergent (but smaller) than for smaller  $n$ .

$D$	$N$	$(n=1)$				
		2	3	4	5	6
2	0.488	0.500	0.493	0.481	0.446	0.429
	5.15	4.62	5.01	5.80	9.84	13.57
3	0.498	0.495	0.510	0.510	0.467	
	4.76	4.83	4.38	4.36	6.94	
4	0.495	0.498	0.510	0.510		
	4.85	4.74	4.36	4.38		
5	0.483	0.505	0.495			
	5.59	4.50	4.79			
6	...	0.455				
		9.74				
7	...					
			$(n=2)$			
2	0.483	0.488	0.495	0.490		
	7.98	7.74	7.16	7.64		
3	0.488	0.483	0.490			
	7.77	8.06	7.47			
4	0.498	0.490				
	7.01	7.56				
5	0.444					
	17.69					
			$(n=3)$			
2	0.476	0.474	0.476			
	11.62	11.67	11.57			
3	0.474	0.476				
	11.68	11.62				
4	...					
			$(n=4)$			
2	0.476	0.476				
	14.41	14.42				
3	0.476					
	14.43					
			$(n=5)$			
2	0.476					
	17.47					

spherical moments, are consistent with the values found from  $\bar{\chi}$ , they are not any better.

A similar analysis was performed on the many different sc and fcc lattice series for the Heisen-

berg model ( $n=0-5$ ,  $\chi$ , and  $\mu_t$  for various  $t$ ). Here it is found that while the two-dimensional series have a large number of singularities in the PA's which are complex, the higher  $R$  derivatives ( $n \geq 2$ ) produce a large number of real ferromagnetic poles. However, these poles have not yet settled down sufficiently for one to claim a convergence. Also calculated were the PA's for the  $R$  derivatives to  $\bar{\chi}^{\text{sc}}$  for the spherical model. These approximants give far fewer real poles (e.g., hardly any for  $n \leq 2$ ). This seems to be an indication that the series for the Heisenberg model ( $D=3$ ) are behaving differently from the spherical model ( $D=\infty$ ) series for which  $T_c=0$ .

For the sc lattice series, the PA's for all the models ( $D=1, 2, 3$ , and  $\infty$ ) show a persistent antiferromagnetic zero. Convergence to the desired physical singularity can sometimes be improved in cases like this by performing a transformation on the series to move the antiferromagnetic singularity farther away from the origin of the complex  $K$  plane ( $K=J_{xy}/k_B T$ ). Since when going from one value of  $n$  to another this spurious singularity moved about considerably, and because the singularity was not found on the fcc lattice series at all, the transformations were not employed extensively.

#### D. Sequences to obtain $\phi T_c/T_c^{\text{MF}}$

Returning to the ratios as plotted in Fig. 1, some interesting sequences can be obtained. Using the expression for the ratios [Eq. (4.6)] ( $\gamma_n$  could be replaced by any of the appropriate scaling exponents) and the scaling hypothesis [Eq. (2.6)], one obtains

$$\rho_{n,l} = (T_c/T_c^{\text{MF}})[(\gamma_0 + n\phi - 1)/l + 1]. \quad (4.8)$$

If  $\rho_{n-1,l}$  is subtracted from  $\rho_{n,l}$  two special sequences are obtained,

$$\Delta_{n,l} \equiv \rho_{n,l} - \rho_{n-1,l} = (\phi T_c/lT_c^{\text{MF}}) + O(1/l^2) \quad (4.9)$$

and

$$l\Delta_{n,l} = l(\rho_{n,l} - \rho_{n-1,l}) = \phi(T_c/T_c^{\text{MF}}) + O(1/l). \quad (4.10)$$

In Fig. 1,  $\Delta_{n,l}$  represents the vertical space between two points on the  $n-1$  and the  $n$ th  $R$ -derivative ratio plots. Even though all pairs of ratio curves are getting closer together ( $\Delta_{n,l}$  getting smaller) as  $l$  increases, only if the scaling hypothesis is true will all the  $\Delta_{n,l}$  sequences have the same exponent  $\phi$  and critical temperature  $T_c$ . The value of  $\Delta_{n,l}$  can be plotted versus  $1/l$ , and the sequence should converge to the origin as  $l \rightarrow \infty$  (note that only if all the  $R$  derivatives produce the same  $T_c$  will this sequence vanish as  $l \rightarrow \infty$ ). Since the intercept of the plot is known precisely to be zero, the slope of the curve can be estimated to give  $\phi T_c/T_c^{\text{MF}}$ .

In Fig. 2, one of our many plots for this type of

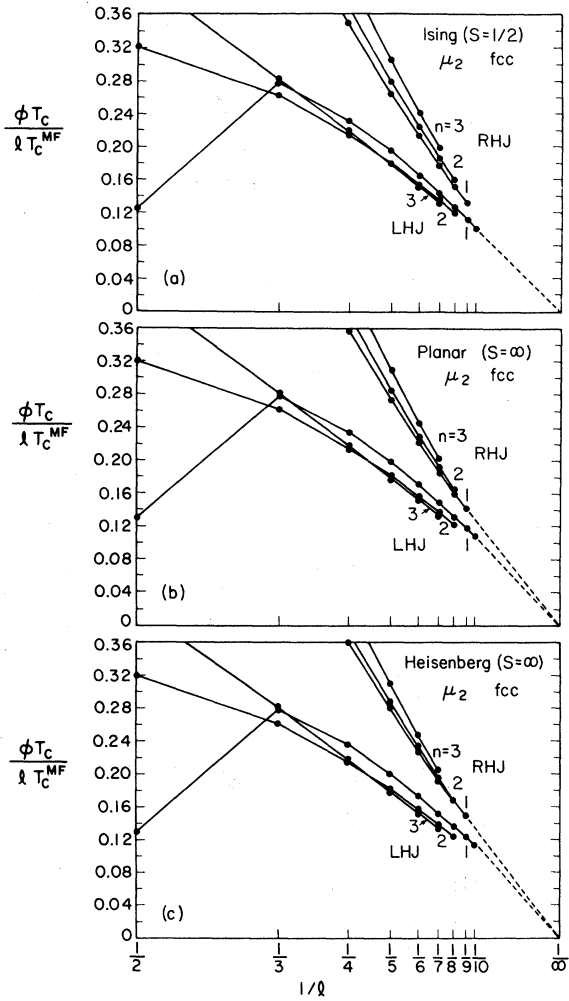


FIG. 2. Sequences shown are given by Eq. (4.9) and should converge to the origin with slope  $\phi T_c/T_c^{MF}$ . The series used are  $\mu_2^{fcc}$  for the (a) Ising, (b) planar, and (c) classical Heisenberg models. The dashed line on the Ising model plots uses the known exact results while the lines on the other models are visual guides only.

sequence is shown. Here again the ambiguity of LHJ and RHJ ratios arises. We believe, though, that since both types of ratios must converge to  $T_c/T_c^{MF}$ , by plotting the sequences for both LHJ and RHJ ratios one can obtain bounds on the limiting slope of the curves. In Fig. 2(a) the sequence of  $\Delta_{n,l}$  for  $\mu_2^{fcc}$  of the Ising model are shown.<sup>31</sup> The dashed line extending from the origin indicates the value of  $\phi T_c/T_c^{MF} = 0.992$ , where we have used  $T_c/T_c^{MF} = 0.5667$  and  $\phi = \gamma_0 = \frac{7}{4}$ .<sup>14</sup>

In Figs. 2(b) and 2(c) are the  $\Delta_{n,l}$  sequences for  $\mu_2^{fcc}$  for the planar and classical Heisenberg models, respectively. The dashed lines in these figures are visual guides for the reader indicating the bounds placed on  $\phi T_c/T_c^{MF}$ . While the LHJ curves

are the most rapidly convergent for the Ising model, the RHJ curves appear to be converging fastest for the Heisenberg model. In fact, the RHJ  $n=1$  and  $n=2$  curves have practically merged at  $\phi T_c/T_c^{MF} \cong 1.4$ . The planar model seems to be indicating its position midway between the Ising and Heisenberg models by placing its limiting slope somewhere between the LHJ and the RHJ plots. Here a value of approximately 1.2 might be a good estimate for the slope  $\phi T_c/T_c^{MF}$ .

Examples of the sequence  $l\Delta_{n,l}$ ,<sup>33</sup> Eq. (4.10), are shown in Fig. 3. These sequences should converge to the intercept  $\phi T_c/T_c^{MF}$ . As shown in the figures, the predictions using the sequence (4.10) on  $\bar{\chi}^{fcc}$  are entirely compatible with the  $\mu_2^{fcc}$  results of sequence (4.9). The Ising model sequences are

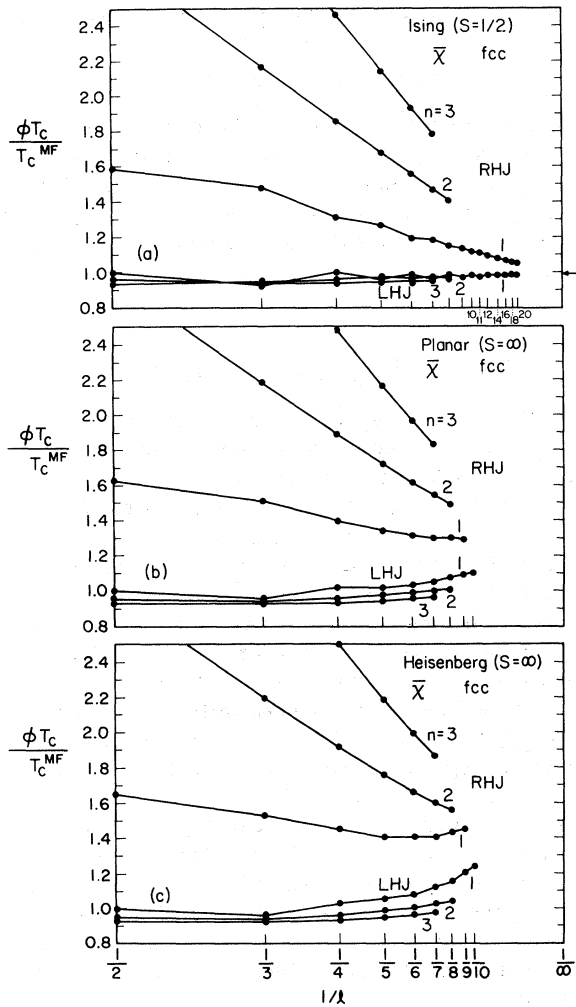


FIG. 3. These curves represent quantities defined by Eq. (4.10) and should converge to the product  $\phi T_c/T_c^{MF}$ . Part (a) uses the Ising model  $\bar{\chi}^{fcc}$  series while (b) and (c) are the planar and Heisenberg models.

shown in Fig. 3(a) where again the LHJ and RHJ notation is used. The longer sequence for  $n=1$  was obtained by using the relationship (3.6) and the 21-term Ising-model square lattice series.<sup>34</sup> Since this entire set of sequences shows very good convergence to the predicted critical values, they serve to demonstrate the validity of the method.

The planar and Heisenberg model results are contained in Figs. 3(b) and 3(c). Again as in the  $\Delta_{n,l}$  sequences, the RHJ curves appear to be giving the best convergence. The curves for the Heisenberg model seem to be turning up slightly, and might appear to be starting to run away; but after examining the  $n=1$  curves closely it is observed that the last points are coming back down. Perhaps the upward curvature is only an indication that the product  $\phi T_c/T_c^{\text{MF}}$  is larger for  $D=3$  than for  $D=2$  or  $D=1$ . The sequences (4.9) and (4.10) show the trends of the results very well even though they are not as rapidly convergent as could be desired.

#### E. Sequence for $T_c/T_c^{\text{MF}}$

In the spirit of Sec. III D, an additional set of sequences was obtained in an attempt to separate the critical temperature from the exponent. Returning to the ratios (4.8), we see that if they are weighted by  $n$  before the differences are taken, an equation for  $T_c/T_c^{\text{MF}}$  is obtained,

$$\begin{aligned} \bar{\Delta}_{n,l} &\equiv n\rho_{n-1,l} - (n-1)\rho_{n,l} \\ &= (T_c/T_c^{\text{MF}})[(\gamma_0 - 1)/l + 1] + O(1/l^2) \end{aligned} \quad (4.11)$$

for all  $n$ . For  $n=0$ ,  $\bar{\Delta}_{n,l}$  is an undefined quantity; when  $n=1$ ,  $\bar{\Delta}_{1,l}$  equals the two-dimensional ratios. For  $n > 1$ , however, the sequence represents a quantity which not only should intersect the  $l = \infty$  axis at  $T_c/T_c^{\text{MF}}$ , but also should approach the intercept with the same slope as the two-dimensional ratios. That is, as  $l \rightarrow \infty$ , the  $\bar{\Delta}_{n,l}$  curves for all  $n$  should become common. The LHJ and RHJ ambiguity again applies except for  $n=1$ , at which point they are the same. Obviously, the sequence is not restricted to the susceptibility series and if we wished to use a different quantity such as  $\mu_t$  then the exponent  $\gamma_0$  would be replaced by the appropriate exponent ( $t\nu_0 + \gamma_0$ ).

Shown in Figs. 4–6 are several of the  $\bar{\Delta}_{n,l}$  sequences plotted versus  $1/l$ . For the Ising model (Fig. 4), we have shown the  $\mu_2^{\text{fcc}}$ ,  $\bar{\chi}^{\text{fcc}}$ ,  $\mu_{-3/4}^{\text{fcc}}$ , and  $\mu_{-3/2}^{\text{fcc}}$  sequences. These values are of particular interest since for  $t=2$  and  $t=0$  ( $\bar{\chi}$ ) the critical exponent indicates a pole. Hence the slopes of the curves,

$$m \equiv (T_c/T_c^{\text{MF}})(t\nu_0 + \gamma_0 - 1), \quad (4.12)$$

are positive. On the other hand, since  $\nu_0 = 1$  and  $\gamma_0 = \frac{7}{4}$  when  $t = t_0 = -\frac{3}{4}$ ,  $t_0\nu_0 + \gamma_0 = 1$  and the slope is zero.

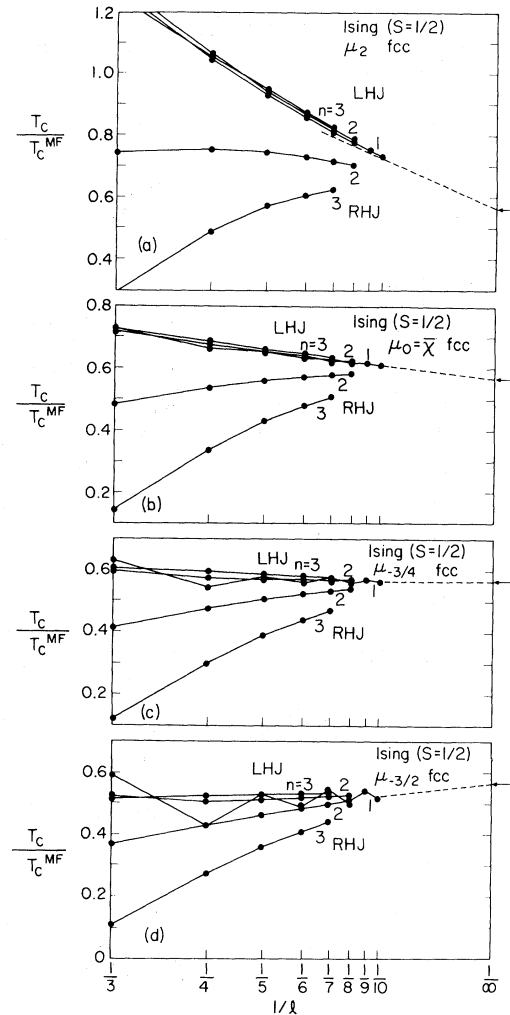


FIG. 4. Sequences of Eq. (4.11) for the Ising model fcc lattice series are shown for the spherical moments [Eq. (1.1)] with  $t=2, 0, -\frac{3}{4}$ , and  $-\frac{3}{2}$  in parts (a), (b), (c), and (d), respectively. The notation LHJ and RHJ refers to how the ratios are plotted and is explained in the text.

These sets of curves are shown in Figs. 4(a)–4(c). In Fig. 4(d),  $t = -\frac{3}{2}$ , and the curves must now point upward (negative slope). The very fact that the slope goes from positive to negative as  $t$  is lowered should serve as evidence for a critical point. The dashed lines shown on these figures represent the predicted limiting slopes using the  $\nu_0$  and  $\gamma_0$  values given above.

In Fig. 5 are the sequences for the planar model. The striking similarity between these plots and those for the Ising model are most apparent for  $t \geq 0$ , but can still be seen for  $t < 0$  (cf. curves for  $t = -\frac{3}{2}$ ). The value of  $t_0$  for the planar model is particularly hard to obtain, but must be somewhere

around  $t_0 = -\frac{3}{2}$ . In Table V the  $n=2$ , LHJ sequences for the Ising and planar models are compared. For the Ising model it appears that the sequence has almost converged to the known value  $T_c/T_c^{MF} = 0.5667$ , but is definitely coming in from above. Using the Ising sequence as a guide, one can see why for the planar model the  $t_0 = -\frac{3}{2}$  sequences seem to be more appropriate than  $t_0 = -\frac{7}{4}$ . Figure 5(d) shows the sequence for  $t = -2$ . Although it is perhaps not visible on the figure, these sequences are just beginning to show upward curvature, indicating that  $t_0 \gtrsim -2$ .

The Heisenberg-model sequences are shown in Fig. 6. While the plots for  $\mu_2$  and  $\bar{\chi}$  are similar to the Ising curves, they are not quite as similar as the planar model plots. As in the  $\Delta_{n,l}$  sequences,

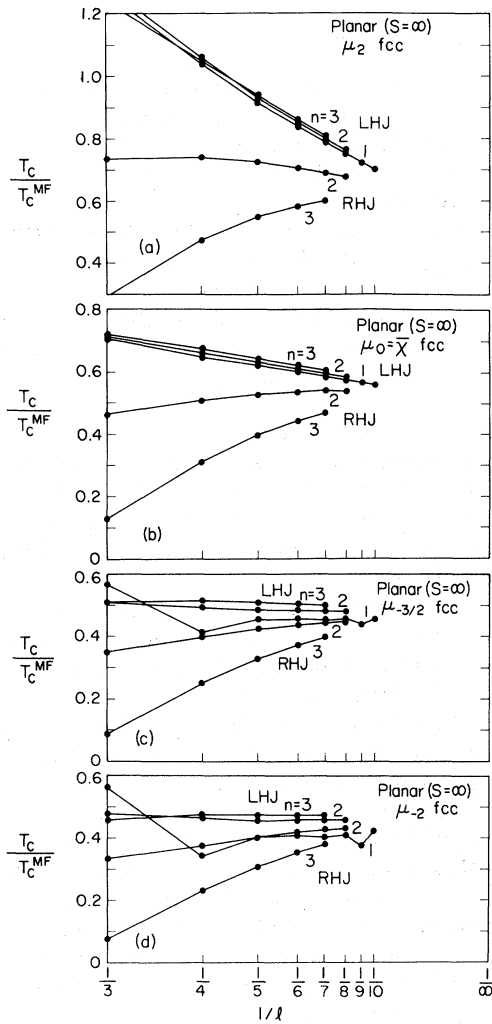


FIG. 5. Sequences of Eq. (4.11) for the classical planar model fcc lattice series are shown for the spherical moments, Eq. (1.1),  $t=2, 0, -\frac{3}{2}$ , and  $-2$  in parts (a), (b), (c), and (d), respectively. The notation LHJ and RHJ is explained in the text.

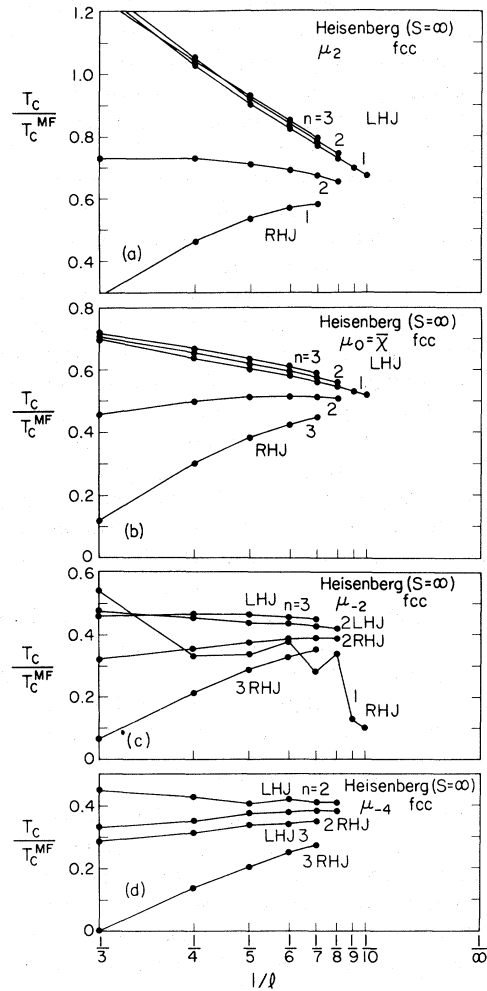


FIG. 6. Sequence of Eq. (4.11) for the classical Heisenberg model fcc lattice series are shown for the spherical moments  $t=2, 0, -2$ , and  $-4$  in parts (a), (b), (c), and (d), respectively. The points for the  $n=1, t=-4$  sequence are oscillatory, as expected, and are therefore not shown. Values of these for  $l=3-10$  are 0.734, 0.133, 0.012, 0.252,  $-21.019$ , 0.229, 1.065, and 0.221.

TABLE V. The sequence for  $n=2$ , LHJ [Eq. (4.11)] is given for some negative spherical moments [Eq. (1.1)]. The Ising-model sequence ( $t=-\frac{3}{2}$ ) should be approaching the known  $d=2$  critical point ( $T_c/T_c^{MF} = 0.5667$ ) with zero slope. The planar model sequences indicate a critical temperature slightly larger than 0.47.

$l$	Ising model		Planar model	
	$t=t_0=-\frac{3}{4}$	$t=-\frac{3}{2}$	$t=-\frac{3}{2}$	$t=-\frac{7}{4}$
1	0.773 05	0.631 02	0.631 02	0.605 87
2	0.567 76	0.443 53	0.443 53	0.412 15
3	0.598 31	0.510 76	0.510 76	0.493 43
4	0.576 22	0.492 83	0.492 83	0.476 11
5	0.572 46	0.484 14	0.484 14	0.468 63
6	0.570 12	0.484 07	0.484 07	0.470 66
7	0.569 76	0.481 52	0.481 52	0.469 03
8	0.569 02	0.480 29	0.480 29	0.468 82

the RHJ  $\Delta_{n,t}$  curves are more appropriate for the Heisenberg model, while the LHJ curves are the choice for the Ising. This is seen in the  $\mu_2$  and  $\bar{\chi}$  plots for the Heisenberg model by the greater distance between the LHJ curves. Also, the  $\mu_2$  case shows a leveling-off behavior for the  $n=2$  RHJ curve, indicating a critical temperature in the vicinity of  $T_c/T_c^{\text{MF}} \sim 0.38$ . While it is impossible to estimate a value for  $t_0$  for the Heisenberg model, we feel that if the series were but two or three terms longer, a great deal more could be told about the existence of a critical point by observing this particular sequence. We have investigated even more negative values of  $t$  for the Heisenberg model and show  $\mu_{-4}$  in Fig. 6(d). For this unusual value of  $t$  the sequence would be expected to be curving upward, indicating a large negative slope, but only in the case of  $n=3$  is this type of behavior seen. This result is not totally surprising, for surely at these large (negative) values of  $t$  the series are simply approximating the nearest-neighbor spin-spin correlation function [see Eq. (1.1) defining  $\mu_t$ ] and are almost independent of  $r$  and hence  $t$ . In fact, it is for this reason that we think the  $n=2$ , RHJ sequence of  $t=-4$  is showing such similarity to the  $n=2$ , RHJ  $t=-2$  sequence.

#### F. Spherical model ( $D=\infty$ )

The susceptibility series  $\bar{\chi}^{\text{sc}}$  for the spherical model were also generated<sup>26</sup> and analyzed, where appropriate, by the methods described. The ratio plots show the well-known downward curvature of the two-dimensional series. Likewise, there is downward curvature for  $n=1$ , and some curvature for  $n=2$ . For the higher  $R$  derivatives ( $n \geq 3$ ) the plots were more like the other models, indicating the lesser ability of these series to show the effects of the Hamiltonian. The PA's to this series were discussed in Sec. III B and, as mentioned there, show differences from the other models for the large  $n$  values. In Fig. 7 we present the sequences for  $\Delta_{n,t}$ . Note how rapidly the sequences turn up (unlike the  $D=1-3$  cases) just before they begin to oscillate wildly.

#### G. "Natural variables"

On the linear chain lattice it has been shown<sup>35</sup> that

$$\bar{\chi} = (1 + y_D)/(1 - y_D), \quad (4.13)$$

where

$$y_D \equiv I_D(DJ/k_B T)/I_{D/2-1}(DJ/k_B T) \quad (4.14)$$

is the  $n$ n correlation function. Here  $I_D(DJ/k_B T)$  is the  $D$ th-order modified Bessel function of the second kind.

For the Ising model ( $D=1$ ), Eq. (4.14) reduces to

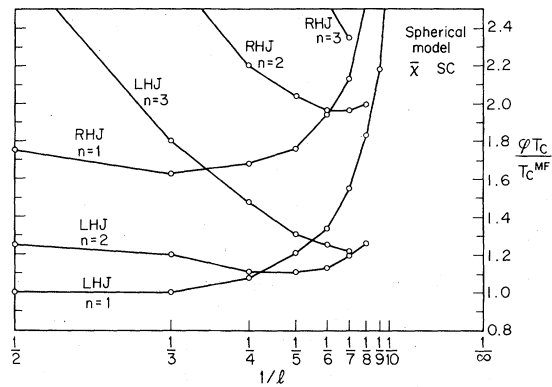


FIG. 7. Spherical model  $\bar{\chi}^{\text{sc}}$  series sequences for  $\phi T_c/T_c^{\text{MF}}$  given by Eq. (4.10). These curves all bend upward and eventually begin to oscillate.

$$y_1 = \tanh(J/k_B T). \quad (4.15)$$

If the Ising-model series are expressed in terms of  $y_1$ , the coefficients on even the higher-dimensional lattices are all integers. Hence the variables  $y_D$  are sometimes referred to as the natural variables. We transformed our  $\bar{\chi}$  and  $\mu_2$  series into a double power series in the natural variables [ $y_D(DJ_{xy}/k_B T)$  and  $y_D(DJ_z/k_B T)$ ] and performed most of the analysis again. While the predictions from these series were consistent with the results of the untransformed series, they were no more revealing.

#### V. CONCLUSIONS

We believe we have completed a thorough analysis of high-temperature series for the two-dimensional quadratic lattice. Through the comparisons of the four spin models ( $D=1, 2, 3$ , and  $\infty$ ) considerable evidence has arisen concerning the possibility of a phase transition.

By employing the concepts of scaling theory and by developing new sequences for the critical indices, we have presented evidence that the two-dimensional planar model has a nonzero critical point. Furthermore, with the aid of the negative spherical moment series and PA's for the higher  $R$  derivatives of all series, we estimate  $T_c/T_c^{\text{MF}} = 0.475 \pm 0.015$ . The new sequences [(4.9) and (4.10)] yield  $\phi T_c/T_c^{\text{MF}} = 1.2 \pm 0.1$ . Then by using the scaling result  $\gamma_n = (n+1)\gamma_0$ , which is rigorous for  $n=1$ , we obtain  $\gamma_0 = 2.53_{-0.28}^{+0.30}$  for the two-dimensional planar model. This value is compatible with Moore's<sup>9</sup> result of  $\gamma_0 = 3.0 \pm 0.5$  for the model but disagrees greatly from the conclusions of Betts, Elliott, and Ditzian for the  $XY$  model<sup>36</sup> ( $\gamma_0 = 1.5 \pm 0.02$ ).

For the classical Heisenberg model ( $D=3$ ) we have obtained both positive and negative evidence concerning the possibility of a phase transition. If we were to argue for a  $T_c$  we would have to point

out the strong similarities between the results of the Heisenberg, planar, and Ising models. Yet in view of the slight upward turn of sequences such as those displayed in Fig. 3, we have to wonder if these series are eventually going to become as dramatic as the spherical model (cf. Fig. 7). Or is this turning upward merely a product of the fact that  $\phi T_c/T_c^{MF}$  is larger for the Heisenberg model than for the Ising model? If we were forced to estimate critical values we might choose  $T_c/T_c^{MF} \approx 0.38$  and  $\phi T_c/T_c^{MF} \approx 1.4$ , and hence obtain  $\gamma_0 \approx 3.5$ , which is compatible with the Ritchie and Fisher<sup>37</sup> estimate of  $3.0 \pm 0.5$ .

#### ACKNOWLEDGMENTS

We wish to thank Dr. L. Liu, Dr. D. Karo, Dr. F. Harbus, Dr. M. H. Lee, Dr. G. Paul, and Dr. R. Krasnow for many helpful discussions and remarks. We acknowledge receipt of a preprint from W. J. Camp, received after completion of the

present work, which raises an interesting possibility for the nature of the low-temperature phase.<sup>38</sup>

#### APPENDIX

The complete set of general- $R$  series for the susceptibility, second moment, and specific heat for the planar and classical Heisenberg models on both the simple-cubic and face-centered-cubic lattices are presented in Ref. 26. Various spherical-moment series for the above models and the spin- $\frac{1}{2}$  Ising model on the face-centered-cubic lattice are also presented.

*Note added in proof.* After the galley proofs of this article were received, we obtained copies of two interesting preprints. In the first of these, J. Zittartz proved that for the case  $d=2$ ,  $D=2$  a phase transition of the Stanley-Kaplan type (Ref. 7) exists. In the second preprint, K. Binder and D. P. Landau performed Monte Carlo calculations on the case  $d=2$ ,  $D=3$  with a range of values of spin anisotropy; their work suggests that a transition of the Stanley-Kaplan type also exists for  $D=3$ .

\*Work forms a portion of the Ph.D. thesis of D. N. L., May 1973, Physics Dept., MIT. Work supported by the National Science Foundation and Air Force Office of Scientific Research. Preliminary accounts of portions of the present work have appeared in D. N. Lambeth and H. E. Stanley, AIP Conf. Proc. **10**, 831 (1973); H. E. Stanley, in *Phase Transitions and Critical Phenomena*, edited by C. Domb and M. S. Green (Academic, London, 1974), Vol. 3, Chap. 2; H. E. Stanley, T. S. Chang, F. Harbus, and L. L. Liu, in *Local Properties near Phase Transitions*, (Proc. 1973 Enrico Fermi Summer School), edited by K. A. Müller (Academic, London, 1975), Chap. 1.

†Present address: Eastman Kodak Physics Research Lab., Kodak Park, Rochester, N. Y.

<sup>1</sup>L. Onsager, Phys. Rev. **65**, 117 (1944).

<sup>2</sup>(a) T. H. Berlin and M. Kac, Phys. Rev. **86**, 821 (1952); (b) H. E. Stanley, *ibid.* **176**, 718 (1968).

<sup>3</sup>V. G. Vaks and A. I. Larkin, Zh. Eksp. Teor. Fiz. **49**, 975 (1965) [Sov. Phys.-JETP **22**, 678 (1966)].

<sup>4</sup>(a) N. D. Mermin and H. Wagner, Phys. Rev. Lett. **17**, 1133 (1966); (b) N. D. Mermin, J. Math. Phys. **8**, 1061 (1967).

<sup>5</sup>P. C. Hohenberg, Phys. Rev. **158**, 383 (1967).

<sup>6</sup>N. N. Bogoliubov, Phys. Abh. Sowjetunion **6**, 1 (1962); **6**, 113 (1962); **6**, 229 (1962).

<sup>7</sup>H. E. Stanley and T. A. Kaplan, Phys. Rev. Lett. **17**, 913 (1966); J. Appl. Phys. **38**, 975 (1967); H. E. Stanley, Phys. Rev. **158**, 546 (1967); **164**, 709 (1967).

<sup>8</sup>H. E. Stanley, Phys. Rev. Lett. **20**, 150 (1968).

<sup>9</sup>M. A. Moore, Phys. Rev. Lett. **23**, 861 (1969).

<sup>10</sup>(a) V. Mubayi and R. V. Lange, Phys. Rev. **178**, 882 (1967); see also R. Kenan, Phys. Rev. B **1**, 3205 (1970); (b) T. Oguchi, Prog. Theor. Phys. **48**, 372 (1972), and references contained therein; (c) K. Yamaji and J. Kondo [J. Phys. Soc. Jpn. **35**, 25 (1973)] claim to have added two terms to the general- $S$  (spin quantum number) series, but actually the first term was reported in H. E. Stanley, J. Appl. Phys. **40**, 1546 (1969); they

emphasize the fact that the series are less regular for small  $S$ .

<sup>11</sup>V. L. Berezhinskii, Zh. Eksp. Teor. Fiz. **59**, 907 (1970) [Sov. Phys.-JETP **32**, 493 (1971)]; **61**, 1144 (1971) [**34**, 610 (1972)]; see also J. M. Kosterlitz and D. J. Thouless, J. Phys. C **5**, L124 (1972).

<sup>12</sup>E. Riedel and F. Wegner, Z. Phys. **225**, 195 (1969).

<sup>13</sup>A. Hankey and H. E. Stanley, Phys. Rev. B **6**, 3515 (1972).

<sup>14</sup>R. Krasnow, F. Harbus, L. L. Liu, and H. E. Stanley, Phys. Rev. B **7**, 370 (1973); see also the preliminary report of F. Harbus, R. Krasnow, L. Liu, and H. E. Stanley, Phys. Lett. A **42**, 65 (1972).

<sup>15</sup>R. Abe, Prog. Theor. Phys. **44**, 339 (1970); M. Suzuki, *ibid.* **46**, 1054 (1971).

<sup>16</sup>J. Oitmaa and I. G. Enting, Phys. Lett. A **36**, 91 (1971); J. Phys. C **5**, 231 (1972); I. G. Enting and J. Oitmaa, Phys. Lett. A **38**, 107 (1972).

<sup>17</sup>D. C. Rapaport, Phys. Lett. A **37**, 407 (1971).

<sup>18</sup>L. L. Liu and H. E. Stanley, Phys. Rev. Lett. **29**, 927 (1972); Phys. Lett. A **40**, 272 (1972); Phys. Rev. B **8**, 2279 (1973). See also the independent work of C. A. W. Citteur and P. W. Kasteleyn, Phys. Lett. A **42**, 143 (1972); Physica **68**, 491 (1973).

<sup>19</sup>The inequalities involve the spin-spin correlation functions and are much more complicated for the  $D > 1$  cases. See R. B. Griffiths, in *Phase Transitions and Critical Phenomena*, edited by C. Domb and M. S. Green (Academic, London, 1972), Vol. 1, Ch. 2.

<sup>20</sup>M. Wortis, D. Jasnow, and M. A. Moore, Phys. Rev. **185**, 805 (1969).

<sup>21</sup>M. Ferer, M. A. Moore, and M. Wortis, Phys. Rev. B **4**, 3954 (1971).

<sup>22</sup>D. N. Lambeth and H. E. Stanley (unpublished); P. M. Horn, R. D. Parks, D. N. Lambeth and H. E. Stanley, Phys. Rev. B **9**, 316 (1974); T. S. Chang, Luke L. Liu, D. N. Lambeth and H. Eugene Stanley, *ibid.* **11**, 1254 (1975).

<sup>23</sup>C. G. Shull, W. A. Strauser, and E. O. Wollan, Phys.

- Rev. 83, 333 (1951); A. J. Guttmann, J. Phys. C 5, 2460 (1972).
- <sup>24</sup>R. J. Birgeneau, H. J. Guggenheim, and G. Shirane, Phys. Rev. Lett. 22, 720 (1969); Phys. Rev. B 1, 2211 (1970).
- <sup>25</sup>M. B. Salamon and H. Ikeda, Phys. Rev. B 7, 2017 (1973).
- <sup>26</sup>For a complete listing of the series see NAPS document #02680 for 46 pages of general- $R$  series. Order from ASIS/NAPS, c/o Microfiche Publications, 305 East 46th Street, New York, N. Y. 10017. Remit with order for each NAPS document number \$1.50 for microfiche or \$5.00 for photocopies for up to 30 pages; 15¢ per page for each additional page over the first 30 pages. Make checks payable to Microfiche Publications.
- <sup>27</sup>F. Harbus and H. E. Stanley, Phys. Rev. B 7, 365 (1973).
- <sup>28</sup>See, for example, H. E. Stanley, *Introduction to Phase Transitions and Critical Phenomena* (Oxford U. P., London, 1971), Chap. 9; and G. Paul and H. E. Stanley, Phys. Rev. B 5, 2578 (1972); 5, 3715 (1972) for the methods used here.
- <sup>29</sup>See, for example, G. A. Baker and D. L. Hunter, Phys. Rev. B 7, 3346 (1973); 7, 3377 (1973).
- <sup>30</sup>In addition, Neville tables and Park's method were studied but did not yield much additional evidence concerning the critical indices.
- <sup>31</sup>The extra term plotted for the  $\bar{\chi}^{(1)}$  series was obtained by using Eq. (2.10). Additional relationships also hold for quantities such as  $\mu_2$  (see Ref. 18).
- <sup>32</sup>The major difference for  $n \geq 2$  is that the Ising model ratios are approaching the intercept with slightly less slope than the ratios of the other models.
- <sup>33</sup>The sequence  $l\Delta_{n,l}$  is the set of slopes measured from the origin to the point  $\Delta_{n,l}$ .
- <sup>34</sup>M. F. Sykes, D. S. Gaunt, P. D. Roberts, and J. A. Wyles, J. Phys. A 5, 624 (1972).
- <sup>35</sup>H. E. Stanley, Phys. Rev. 179, 570 (1969).
- <sup>36</sup>D. D. Betts, C. J. Elliott, and R. V. Ditzian, Can. J. Phys. 49, 1327 (1971).
- <sup>37</sup>See D. S. Ritchie, Ph.D. thesis (Cornell, Ithaca, 1973) (unpublished); see also D. S. Ritchie and M. E. Fisher, AIP Conf. Proc. 5, 1245 (1973).
- <sup>38</sup>W. J. Camp and J. Van Dyke, J. Phys. C 8, 336 (1975).